ChemComm

Photocatalytic hydrogen evolution on Si photocathodes modified with bis(thiosemicarbazonato)nickel(II)/Nafion

Journal:	*ChemComm*
Manuscript ID	CC-COM-05-2019-004117.R1
Article Type:	Communication

COMMUNICATION

Photocatalytic hydrogen evolution on Si photocathodes modified with bis(thiosemicarbazonato)nickel(II)/Nafion

Received 00th May 2019,
Accepted 00th June 2019

DOI: 10.1039/x0xx00000x

Saumya Gulati,[a] Oleksandr Hietsoi,[b] Caleb A. Calvary,[b] Jacob M. Strain,[a] Sahar Pishgar,[a] Henry C. Brun,[b] Craig A. Grapperhaus,[b] Robert M. Buchanan,*[b] and Joshua M. Spurgeon*[a]

The molecular catalyst diacetyl-bis(N-4-methyl-3-thiosemicarbazonato) nickel(II) (NiATSM) was integrated with Si for light-driven hydrogen evolution from water. Compared to an equivalent loading of Ni metal, the NiATSM/p-Si electrode performed better. Durability of the surface-bound catalyst under operation in acid was achieved without covalent attachment by using Nafion binding.

Cost-effective, scalable hydrogen production from water-splitting is a grand challenge in the field of clean energy. By coupling the electrolysis to light absorption via artificial photosynthesis, the intermittent energy of sunlight can be captured as H_2 fuel.[1] While platinum remains the state-of-the-art catalyst for the hydrogen evolution reaction (HER) at the cathode, numerous other catalysts have been studied.[2]

Molecular catalysts for HER have certain advantages, including low loadings of non-platinum group metal elements, and thus relatively low cost and high abundance. Moreover, the ligand structures can be tailored to tune the active site energetics for activity and selectivity without the constraints imposed by an extended solid lattice in heterogeneous catalysts.[3-5] Molecular HER catalysts based on cobalt,[6-8] iron,[9, 10] molybdenum,[11-13] and nickel[14-16] have been the most common. Molecular Ni complexes are among the most active, such as the well-known DuBois' nickel-bis(diphosphine) catalysts.[17, 18] More recently, we and others have explored a novel monomeric Ni(II) complex of diacetyl-bis(N-4-methyl-3-thiosemicarbazonato), or NiATSM, for its role as a ligand-assisted, metal-centered HER electrocatalyst (Fig. 1).[19] The structures of bis(thiosemicarbazones) (BTSCs) are easily modified and usually synthesized in high yields from inexpensive organic reagents, making them attractive platforms for the design of new HER electrocatalysts. In addition, BTSC ligands are redox non-innocent and can function as a reservoir for charge with hydrogen evolution at either the metal or the ligand.

There have been a number of studies to leverage molecular HER catalysts for solar H_2 generation by incorporating these structures onto the surface of semiconductor photocathodes.[4, 20, 21] In many cases, the catalyst was immobilized on the semiconductor surface via covalent linking strategies for direct charge transfer between the electrode and catalyst.[4, 22, 23] Covalent attachment is often necessary to prevent catalyst delamination or dissolution in aqueous media but adds processing complexity as well as charge-transfer resistance at the interface. Ideally then, a molecular catalyst could be durably coupled to a photoelectrode with low overpotential in aqueous

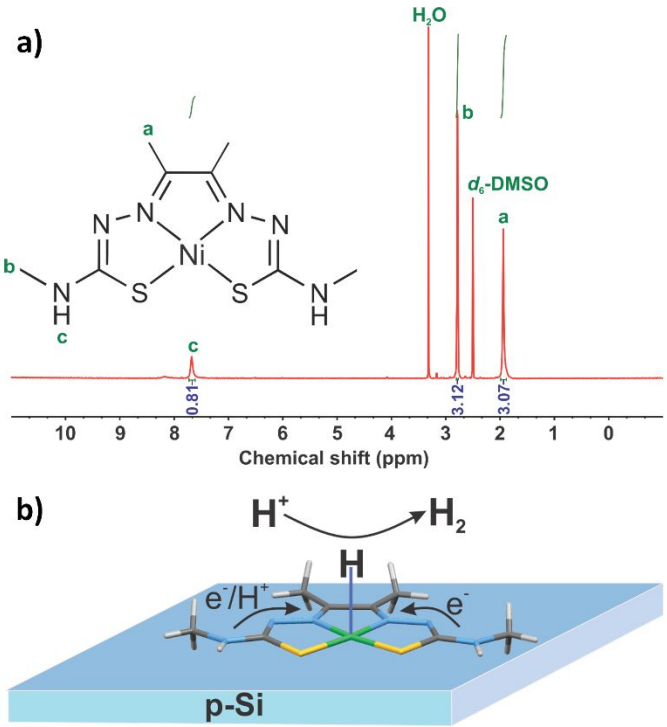

Fig. 1. (a) ^{1}H NMR of NiATSM (500 MHz, d_6-DMSO): 7.69 (1H, br. s), 2.75 (3H), 1.94 (3H, s). (b) Representation of ligand-assisted, metal-centered HER electrocatalysis by NiATSM on p-Si (Nafion not shown).

[a] Conn Center for Renewable Energy Research, University of Louisville, Louisville, Kentucky, 40292, USA. E-mail: joshua.spurgeon@louisville.edu
[b] Department of Chemistry, University of Louisville, 2320 South Brook Street, Louisville, Kentucky 40292, USA. E-mail: robert.buchanan@louisville.edu
Electronic Supplementary Information (ESI) available: [details of any supplementary information available should be included here]. See DOI: 10.1039/x0xx00000x

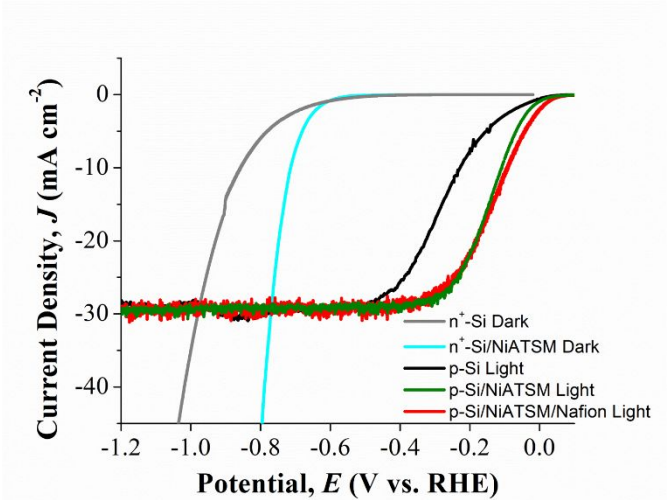

Fig. 2. Current density vs. potential (*J-E*) behavior for electrodes in H_2-saturated 1 M H_2SO_4. Dark electrocatalytic behavior for n^+-Si with and without NiATSM catalyst and illuminated 1 Sun AM1.5 behavior for p-Si photocathodes with and without NiATSM catalyst.

solution at low or high pH where electrolysis efficiency is maximized. NiATSM co-catalyst with CdS nanorods was recently reported for light-driven hydrogen evolution using monochromatic illumination with a sacrificial species at moderate pH values.[24] Herein we report the characterization of the NiATSM catalyst under conditions for practical solar hydrogen generation. Simple catalyst attachment methods were used with p-Si photocathodes in pH 0 aqueous electrolyte to yield robust photoelectrochemical energy-conversion behavior that clearly outperforms an equivalent loading of Ni metal catalyst.

NiATSM was synthesized following previously reported methods[25, 26] and the complex was characterized by NMR (Fig. 1a), elemental analysis, FT-IR (Fig. S1), and UV/vis spectroscopy (Fig. S2). NiATSM is known to be a robust HER homogeneous catalyst in organic solutions, and insoluble in 1 M H_2SO_4.[19, 27] NiATSM was loaded to ~60 nmol cm^{-2} onto Si photoelectrodes as described in the ESI. Fig. 2 shows the photoelectrochemical energy-conversion behavior of NiATSM-coated p-Si photocathodes in 1 M H_2SO_4. Degenerate n^+-Si electrodes were measured as well to test the behavior of the electrodes in the absence of the photoelectrochemical diode, which instead yields ohmic behavior and permits the measurement of dark electrocatalytic Butler-Volmer HER kinetics on the Si substrate. The onset potential and the potential for each electrode at a standard 10 mA cm^{-2} is reported in Table 1. The resulting HER overpotential for the bare n^+-Si was 860 mV, while 1 Sun-illuminated bare p-Si had a potential of -0.220 V vs. RHE, indicating a typical photovoltage from these electrodes of ~640 mV. With the inclusion of the molecular catalyst layer, the n^+-Si/NiATSM overpotential decreased to 712 mV, a decrease of 148 mV relative to the bare n^+-Si. Under illumination, the p-Si/NiATSM potential at 10 mA cm^{-2} was -0.080 V vs. RHE. This represents a shift of 140 mV from the illuminated bare p-Si and is consistent with the observed catalytic shift on photo-inactive substrates.

Durability of the drop-cast NiATSM catalyst layer was investigated with extended potentiostatic operation under

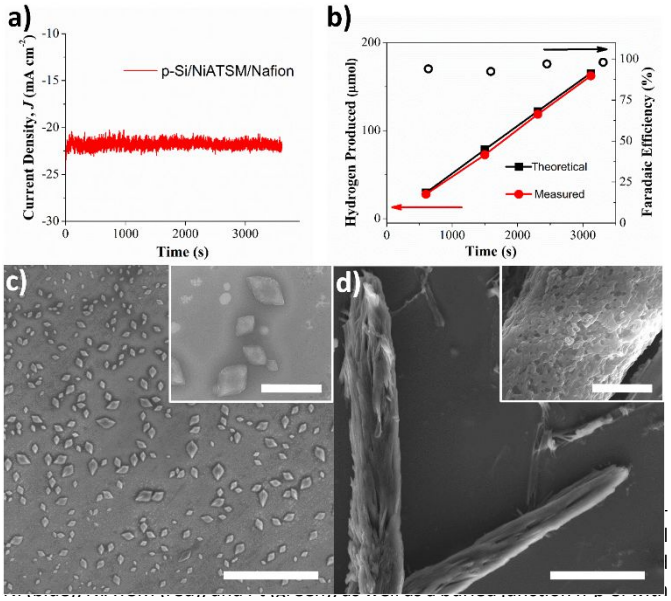

Fig. 3. (a) Current density vs. time at -0.2 V vs. RHE under 1 Sun AM1.5 illumination in 1 M H_2SO_4. (b) Calculated vs. measured H_2 produced by illuminated p-Si/NiATSM/Nafion at -0.2 V vs. RHE in N_2-bubbled 1 M H_2SO_4. SEM images of the p-Si/NiATSM/Nafion electrode (c) before and (d) after the stability measurement in (a). Scale bars correspond to 40 μm and 2 μm for the inset.

illumination at -0.2 V vs. RHE, a potential with a notable initial difference in current density between p-Si/NiATSM and bare p-Si. The p-Si/NiATSM current density vs. potential (*J-E*) behavior declined after this extended potentiostatic measurement back to the approximate behavior of bare p-Si (Fig. S3). This response indicates that the molecular catalyst, which is not covalently attached to the Si surface, may be dislodged under extended operation and generation of H_2 bubbles at the surface. However, by casting the NiATSM layer in a dilute Nafion solution (see ESI) as a cation-exchanging binder, the extended current density vs. time performance became steady at ~22 mA cm^{-2} at -0.2 V vs. RHE over the measured period (Fig. 3a), with consistent *J-E* behavior (Fig. S4). Other than promoting adhesion, the Nafion binder had little effect on the initial energy-conversion behavior of the photocathodes (Fig. 2, Table 1, and Fig. S5). Furthermore, characterization of the H_2 faradaic efficiency by gas chromatography (see ESI) displayed almost total direction of the charge to HER (Fig. 3b). SEM images of the as-deposited NiATSM/Nafion layer on p-Si show that the catalyst formed 1 – 5 μm crystalline particles in the Nafion film (Fig. 3c). After extended potentiostatic operation, however, these particles were observed to agglomerate into larger rod-like particles, some as long as ~ 100 μm (Fig. 3d). We have previously reported the structural rearrangement and stacking interactions of NiATSM under cathodic cycling, and the observed agglomeration here is attributed to similar structural behavior after the passing of significantly more charge.[27] EDS mapping showed that the Ni and S of the initial catalyst was confined to this larger agglomerate particle, with Nafion along the rod edges (Fig. S6).

A common challenge for molecular catalysis researchers is to ensure that the observed electrocatalytic activity is attributable to the molecular structure of the ligand-modified

metal center rather than direct heterogeneous catalysis of the metal atoms left behind after decomposition of the organic framework. Our previously reported X-ray photoelectron spectroscopy (XPS) data on the Ni 2p and S 2p orbitals of the NiATSM catalyst before and after cathodic current cycling in strongly acidic aqueous electrolyte indicates that the molecular structure does not significantly decompose.[27] XPS measurements for the NiATSM on p-Si show similar behavior. Though complicated by the presence of the thin Nafion layer, the XPS data indicated that there was no shift in the Ni oxidation state of the catalyst after the 1 h stability measurement (Figs. S7-9). For NiATSM, this conclusion was further tested by measuring p-Si photocathodes with Ni^0 metal electrodeposited at various loadings. With relatively thick Ni loading (430 nmol cm^{-2}, corresponding to a 35% decrease in the light-limited photocurrent due to parasitic absorption), the illuminated p-Si/Ni potential at 10 mA cm^{-2} was -0.080 V vs. RHE (Fig. S10). The Ni-metal-catalyzed potential gradually decreased to -0.180 V vs. RHE for a loading of 60 nmol cm^{-2}, which is the matching loading of Ni atoms calculated to be present in the NiATSM catalyst layer. The photoelectrochemical behavior of p-Si photocathodes for equivalent molar loadings of metallic Ni and NiATSM is shown in Fig. 4 with a 100 mV improvement in overpotential at 10 mA cm^{-2} for the molecular catalyst relative to the pure metal. The enhanced activity of NiATSM relative to Ni nanoparticles may be attributed to metal-ligand cooperativity during catalysis.[28] In addition to the beneficial contribution of the BTSC ligands to promoting the HER mechanism, the enhancement of the molecular catalyst could be partially attributed to greater access of the electrolyte to each Ni site in the NiATSM molecule compared to the metal Ni deposits.

Table 1. Photoelectrochemical energy-conversion parameters.

Electrode	Onset Potential (V vs. RHE)	Potential at 10 mA cm^{-2} (V vs. RHE)
n^+-Si	-0.670	-0.860
n^+-Si/NiATSM	-0.630	-0.712
p-Si	-0.060	-0.220
p-Si/NiATSM	-0.020	-0.080
p-Si/NiATSM/Nafion	0.006	-0.080
p-Si/Ni[a]	-0.024	-0.180
p-Si/Pt[b]	0.124	-0.012
n^+p-Si/NiATSM	0.170	0.025

[a] Electrodeposited Ni at 60 nmol cm^{-2} to match the loading of NiATSM.
[b] Pt deposited by electroless deposition (see ESI).

The behavior of electrolessly deposited Pt on a p-Si photocathode is also included in Fig. 4 for a comparison of the NiATSM to the state-of-the-art HER catalyst. As expected, the Pt-catalyzed electrode displayed the more efficient energy-conversion behavior, but it only reduced the overpotential by 68 mV at 10 mA cm^{-2} relative to NiATSM (Table 1). Notably, the Pt loading is difficult to control by galvanic displacement and the reduced light-limited current density of the p-Si/Pt curve indicates a significantly heavier catalyst loading in this case as well. Furthermore, forming an n^+p-Si buried homojunction before NiATSM deposition led to even better performance. In this case, a solid-state diode was produced by heavily doping a thin (~ 300 nm) n-type emitter layer at the surface before attachment of the NiATSM for aqueous HER (see ESI). The 105 mV increase for the buried junction at 10 mA cm^{-2} relative to the p-Si/NiATSM/Nafion semiconductor/liquid junction case can be attributed to improved interfacial energetics, increased band bending, and reduced recombination in the p-Si depletion region for a buried junction, as has been demonstrated before for Si photocathodes.[29] The enhanced HER activity thus comes from the improved photovoltage of the Si buried junction, rather than increased NiATSM activity, and is included to show how Si/NiATSM photocathodes could be improved. The photoelectrochemical energy-conversion behavior for bare n^+p-Si is shown in Fig. S11 and the time-dependent photocurrent at -0.2 V vs. RHE of n^+p-Si/NiATSM/Nafion is shown in Fig. S12.

Conclusions

Molecular NiATSM complex was used as a co-catalyst with planar p-Si for photocathodic hydrogen evolution without covalent surface attachment. The addition of Nafion binder during drop-casting was shown to promote catalyst adhesion and steady potentiostatic operation without degradation of the electrochemical energy-conversion performance. The p-Si/NiATSM/Nafion photocathodes produced H_2 with near unity faradaic efficiency. Moreover, the photoelectrode with Ni molecular catalyst displayed a potential 100 mV more positive than an electrode with an equivalent molar loading of Ni metal, demonstrating the benefit of the BTSC ligands for promoting HER by the ligand-assisted, metal-centered mechanism previously described for NiATSM.[19]

Conflicts of interest

There are no conflicts to declare.

Acknowledgements

The authors acknowledge support from the Conn Center for Renewable Energy Research at the University of Louisville. This research was also supported in part by the United States National Science Foundation CHE-1665136 and CHE-1800245.

Notes and references

1. N. S. Lewis and D. G. Nocera, *Proc. Natl. Acad. Sci. U. S. A.*, 2006, **103**, 15729-15735.
2. C. C. L. McCrory, S. Jung, I. M. Ferrer, S. M. Chatman, J. C. Peters and T. F. Jaramillo, *J. Am. Chem. Soc.*, 2015, **137**, 4347-4357.
3. T. D. N. Minh, A. Ranjbari, L. Catala, F. Brisset, P. Millet and A. Aukauloo, *Coord. Chem. Rev.*, 2012, **256**, 2435-2444.
4. N. Queyriaux, N. Kaeffer, A. Morozan, M. Chavarot-Kerlidou and V. Artero, *J. Photoch. Photobio. C.*, 2015, **25**, 90-105.
5. R. Brimblecombe, G. C. Dismukes, G. F. Swiegers and L. Spiccia, *Dalton Trans.*, 2009, 9374-9384.

6. F. Zhao, J. Zhang, T. Abe, D. Wohrle and M. Kaneko, *J. Mol. Catal. A-Chem.*, 1999, **145**, 245-256.
7. E. Deponti, A. Luisa, M. Natali, E. Iengo and F. Scandola, *Dalton Trans.*, 2014, **43**, 16345-16353.
8. Q. X. Peng, D. Xue, L. F. Yang and S. Z. Zhan, *Int. J. Hydrogen Energy*, 2017, **42**, 16428-16435.
9. S. K. Ibrahim, X. M. Liu, C. Tard and C. J. Pickett, *Chem. Commun.*, 2007, 1535-1537.
10. H. J. Lv, T. P. A. Ruberu, V. E. Fleischauer, W. W. Brennessel, M. L. Neidig and R. Eisenberg, *J. Am. Chem. Soc.*, 2016, **138**, 11654-11663.
11. Y. D. Hou, B. L. Abrams, P. C. K. Vesborg, M. E. Bjorketun, K. Herbst, L. Bech, A. M. Setti, C. D. Damsgaard, T. Pedersen, O. Hansen, J. Rossmeisl, S. Dahl, J. K. Norskov and I. Chorkendorff, *Nature Materials*, 2011, **10**, 434-438.
12. B. Seger, K. Herbst, T. Pedersen, B. Abrams, P. C. K. Vesborg, O. Hansen and I. Chorkendorff, *J. Electrochem. Soc.*, 2014, **161**, H722-H724.
13. L. R. Webster, S. K. Ibrahim, J. A. Wright and C. J. Pickett, *Chem-Eur J*, 2012, **18**, 11798-11803.
14. A. Le Goff, V. Artero, B. Jousselme, P. D. Tran, N. Guillet, R. Metaye, A. Fihri, S. Palacin and M. Fontecave, *Science*, 2009, **326**, 1384-1387.
15. D. H. Pool and D. L. DuBois, *J. Organomet. Chem.*, 2009, **694**, 2858-2865.
16. C. F. Wise, D. Liu, K. J. Mayer, P. M. Crossland, C. L. Hartley and W. R. McNamara, *Dalton Trans.*, 2015, **44**, 14265-14271.
17. V. Artero and J. M. Saveant, *Energy Environ. Sci.*, 2014, **7**, 3808-3814.
18. D. L. DuBois, *Inorg. Chem.*, 2014, **53**, 3935-3960.
19. R. Jain, A. Al Mamun, R. M. Buchanan, P. M. Kozlowski and C. A. Grapperhaus, *Inorg. Chem.*, 2018, **57**, 13486-13493.
20. C. L. Hartley, R. J. DiRisio, M. E. Screen, K. J. Mayer and W. R. McNamara, *Inorg. Chem.*, 2016, **55**, 8865-8870.
21. W. R. McNamara, Z. J. Han, C. J. Yin, W. W. Brennessel, P. L. Holland and R. Eisenberg, *Proc. Natl. Acad. Sci. U. S. A.*, 2012, **109**, 15594-15599.
22. A. Krawicz, J. H. Yang, E. Anzenberg, J. Yano, I. D. Sharp and G. F. Moore, *J. Am. Chem. Soc.*, 2013, **135**, 11861-11868.
23. J. Seo, R. T. Pekarek and M. J. Rose, *Chem. Commun.*, 2015, **51**, 13264-13267.
24. W. X. Jiang, Z. L. Xie and S. Z. Zhan, *Inorg. Chem. Commun.*, 2019, **102**, 5-9.
25. H. M. Betts, P. J. Barnard, S. R. Bayly, J. R. Dilworth, A. D. Gee and J. P. Holland, *Angew. Chem.-Int. Edit.*, 2008, **47**, 8416-8419.
26. P. J. Blower, T. C. Castle, A. R. Cowley, J. R. Dilworth, P. S. Donnelly, E. Labisbal, F. E. Sowrey, S. J. Teat and M. J. Went, *Dalton Trans.*, 2003, 4416-4425.
27. A. J. Gupta, N. S. Vishnosky, O. Hietsoi, Y. Losovyj, J. Strain, J. Spurgeon, M. S. Mashuta, R. Jain, R. M. Buchanan, G. Gupta and C. A. Grapperhaus, *Inorg. Chem.*, 2019, Submitted.
28. M. D. Wodrich and X. L. Hu, *Nat. Rev. Chem.*, 2018, **2**.
29. S. W. Boettcher, E. L. Warren, M. C. Putnam, E. A. Santori, D. Turner-Evans, M. D. Kelzenberg, M. G. Walter, J. R. McKone, B. S. Brunschwig, H. A. Atwater and N. S. Lewis, *J. Am. Chem. Soc.*, 2011, **133**, 1216-1219.